Ab initio Ti-Zr-Ni phase diagram predicts stability of icosahedral TiZrNi quasicrystals

R. G. Hennig
Ohio State University, Department of Physics, Columbus, Ohio 43210, USA

A. E. Carlsson and K. F. Kelton
Department of Physics, Washington University, St. Louis, Missouri 63130, USA

C. L. Henley
Laboratory of Atomic and Solid State Physics, Cornell University, Ithaca, New York 14853, USA
(Received 5 October 2004; published 4 April 2005)

The *ab initio* phase diagram determines the energetic stability of the icosahedral TiZrNi quasicrystal. The complete *ab initio* zero-temperature ternary phase diagram is constructed from the calculated energies of the elemental, binary and ternary Ti-Zr-Ni phases. For this, the icosahedral *i*-TiZrNi quasicrystal is approximated by periodic structures of up to 123 atoms/unit cell, based on a decorated-tiling model [R. G. Hennig, K. F. Kelton, A. E. Carlsson, and C. L. Henley, Phys. Rev. B **67**, 134202 (2003)]. The approximant structures containing the 45-atom Bergman cluster are nearly degenerate in energy, and are all energetically stable against the competing phases. It is concluded that *i*-TiZrNi is a ground-state quasicrystal, as it is experimentally the low-temperature phase for its composition.

DOI: 10.1103/PhysRevB.71.144103 PACS number(s): 61.44.Br, 71.15.Nc, 81.30.Bx

I. INTRODUCTION

Thermodynamically stable, long-range ordered quasicrystals of icosahedral symmetry are known in both of the main structural classes of quasicrystal, the Al-transition metal class[1] [e.g., *i*-AlPdMn (Refs. 2–4)] and the Frank-Kasper class[5] [e.g., *i*-ZnMgY (Refs. 6 and 7)]. The Ti-based quasicrystals such as *i*-TiCrSiO (Refs. 8–10) and the thermally stable *i*-TiZrNi (Refs. 11–13) fall into either respective class. The *i*-TiZrNi quasicrystal is of technological interest[14] due to its large hydrogen storage capacity[15] but is less studied than the stable Al-based quasicrystals because of its small grain size.

Experiments on TiZrNi show a periodic crystal structure *W*-TiZrNi, stable at high temperatures which upon cooling undergoes a reversible phase transition at 570 °C to the *i*-TiZrNi quasicrystal.[16] The *W*-TiZrNi phase is a "periodic approximant" of the *i*-TiZrNi quasicrystal, meaning that the unit cell is identical to a fragment of the icosahedral phase.[17] Long-time anneals (up to one month) at 500 °C gave no indication that the *i*-TiZrNi quasicrystal transforms to some other phase. The transformation from *W*-TiZrNi to *i*-TiZrNi demonstrates that the icosahedral phase is lower in energy than the high-temperature *W*-TiZrNi phase.[12,18] The situation here contrasts with the Al-transition metal class, in which the analogous crystal α-AlMnSi (known as "1/1 approximant"), is lower in energy than the quasicrystal of identical composition.

In this work, we show that the *i*-TiZrNi quasicrystal (or a large unit cell crystal of nearly identical structure) is in fact a ground state. We determine the ternary ground-state phase diagram from *ab initio* energy calculations of 45 elemental, binary, and ternary crystalline phases in the Ti-Zr-Ni alloy system. The cohesive energy of the *i*-TiZrNi quasicrystal is estimated from eight different periodic approximants with 81 to 123 atoms per unit cell. The atomic structure of these approximants is given by our previously reported structure model, which is formulated as an atomic decoration of canonical cell tilings, and was fit to a combination of diffraction data and *ab initio* relaxations.[11]

Section II describes the *ab initio* method. In Sec. III *ab initio* relaxations determine the energies and structures of the crystalline Ti-Zr-Ni phases and allow the construction of the ground-state phase diagram. Comparing the calculated energies and lattice parameters to experiments provides a measure of the accuracy of the *ab initio* method. Section IV is the core of the paper; the energy of the quasicrystalline phase is estimated and found to be lower than the energy of the competing crystalline phase. Combining this result with the experimental findings that the quasicrystal is lower in energy than *W*-TiZrNi it is concluded that the quasicrystal is the ground state for its composition. The stability of the approximants and the quasicrystal are explained in terms of the local atomic structure and the resulting electronic density of states.

II. METHOD

Our *ab initio* total energy calculations are performed with VASP,[19,20] a density functional code using a plane-wave basis and ultrasoft Vanderbilt type pseudopotentials.[21,22] The generalized gradient approximation by Perdew and Wang is used.[23] A plane-wave kinetic-energy cutoff of 400 eV ensures convergence of the energy to 1 meV/atom. The *k*-point meshes for the different structures are chosen to guarantee the same accuracy. For Ti and Zr we treat the 3*p* states as valence states in addition to the usual 4*s* and 3*d* states to give an accurate treatment of the interaction at close interatomic distances.

The positions of the atoms, as well as the shape and volume of the unit cells, are relaxed by a conjugate gradient method until the total electronic energy changes by less than

1 meV. This corresponds to atomic-level forces $F_{\max} \leqslant 20$ meV/Å and stresses $\sigma_{\max} \leqslant 50$ MPa. The calculations for the elemental Ni phases are performed spin polarized as these are experimentally the only magnetic phases in the Ti-Zr-Ni system.

For all phases, the cohesive energy is determined from the *ab initio* energies by using the free Ti, Zr, and Ni atom as references. The energy of the free atoms is calculated spin polarized using a cubic cell of 14 Å size. For the alloy phases the heats of formation H_f are given by the energy difference between the alloy phase and the ground-state energy of the elemental phases of the constituent atoms.

The ground-state phase diagram is constructed by calculating the ground-state energy surface from the cohesive energies of the phases. This corresponds to determining the convex hull of the set of energy points as a function of the composition. First, for each concentration the lowest-energy structure is determined. Second, the convex hull of these points is constructed by considering chemical equilibria between the lowest energy phases at different compositions.

The density of states is calculated using a dense *k*-point mesh using a two-step approach. First, an accurate charge density is generated by a self-consistent calculation using a smaller *k*-point grid. In the second step the charge density and thus the effective potential are kept fixed and the eigenvalues are calculated for a dense *k*-point mesh. The density of states is calculated from the eigenvalues by the tetrahedron method.[24]

III. TI-ZR-NI CRYSTALLINE PHASE DIAGRAM

The energies and relaxed structures of elemental, binary, and ternary phases are calculated. The energies and lattice parameters are compared to experimental data to establish the accuracy of the *ab initio* calculations. From the energies the complete ternary ground-state phase diagram is constructed.

The set of structures consists of all TiZrNi phases described in Pearson's *Handbook of Crystallographic Data*[25] and additional hypothetical phases with common intermetallic structures. In particular, we calculate the energies of Ti-Ni phases with structures corresponding to Zr-Ni phases and vice versa since Ti and Zr are chemically similar. Several ternary TiZrNi phases are known. Since the *i*-TiZrNi quasicrystal forms at low Ni concentrations we only investigate ternary TiZrNi structures with Ni concentrations of less than 50%. From the resulting energies of the 45 elemental, binary and ternary crystalline phases the ground state phase diagram is determined.

There are a number of earlier calculations for the Ti-Zr-Ni alloy system all of which concentrated on specific parts of the phase diagram. Several studies investigate the structure of Ti and Zr under pressure because of the pressure-induced martensitic transformations in these elemental systems.[26–28] For the alloys, the Ti-Ni system received particular attention because of the observed shape-memory effect in the TiNi alloy, while only few theoretical studies were performed for intermetallic Zr-Ni phases and ternary Ti-Zr-Ni structures. For the TiNi martensite, *ab initio* calculations with the full-potential linear muffin-tin orbital (FP-LMTO) method chose the correct structure from several conflicting experimental studies[29] and *ab initio* force-constant calculations determined the phonon spectra of the martensite and austenite phase.[30] The Ti-Ni *c*-*T* phase diagram was studied by cluster expansion methods based on LMTO energy calculations.[31] The structure of the ternary TiZrNi *C*14 Laves phases was determined by a combination of *ab initio* calculations and Rietveld refinement of diffraction data.[32]

TABLE I. Structures and cohesive energies of the elemental Ti, Zr, and Ni phases. Wherever available, experimental values are given in parentheses for the cohesive energy (Ref. 33) and the lattice parameters (Ref. 25). The number of *k* points in the irreducible Brillouin zone is indicated by N_k.

Phase	Space group	N_k	E_{coh} in eV/atom	Lattice constants in Å
α-Ti[a]	$P6_3/mmc$	400	5.171 (4.844)	$a=2.948$ (2.951)
				$c=4.665$ (4.686)
ω-Ti[a]	$P6/mmm$	216	5.176	$a=4.590$
				$c=2.842$
β-Ti[b]	$Im\bar{3}m$	322	5.063 (5.004)	$a=3.263$ (3.307)
γ-Ti	$Fm\bar{3}m$		5.113	$c=4.123$
α-Zr[a]	$P6_3/mmc$	672	6.348 (6.299)	$a=3.238$ (3.232)
				$c=5.189$ (5.148)
ω-Zr[a]	$P6/mmm$	528	6.348	$a=5.059$ (5.036)
				$c=3.153$ (3.109)
β-Zr[b]	$Im\bar{3}m$	816	6.276 (6.258)	$a=3.580$ (3.609)
γ-Zr	$Fm\bar{3}m$	770	6.311	$a=4.538$
γ-Ni[c]	$Fm\bar{3}m$	770	4.869 (4.439)	$a=3.532$ (3.523)
α-Ni	$P6_3/mmc$	576	4.845	$a=2.495$
				$c=4.098$
β-Ni	$Im\bar{3}m$	969	4.773	$a=2.803$

[a]The α and ω phase in Ti and Zr are nearly degenerate in energy. For Ti, extrapolation of the experimental *T*-*p* phase diagram (Ref. 34) indicates ω to be the ground-state phase.
[b]Experimentally observed high-temperature phase.
[c]Experimentally observed ground-state phase.

A. Elemental Ti, Zr, and Ni phases

Table I shows the cohesive energies and lattice parameters of the elemental Ti, Zr, and Ni phases. The group IV(b) transition metals Ti and Zr show several phases as a function of pressure and temperature. At high temperatures the β (bcc) phase is stable which upon cooling transforms into the α (hcp) structures. Under pressure the α phase transforms into the ω (hexagonal) phase.[36] For both Ti and Zr the crystal structures at 0 K have not been determined experimentally. However, extrapolation of the $\alpha-\omega$ phase boundary[34] in Ti indicates ω as the ground-state phase. Free energy calculations of α and ω within the quasiharmonic approximation using a tight-binding model show that the α phase is stabilized at ambient temperature by phonon entropy.[37] Our *ab*

initio calculations show in agreement with experiments[34] and earlier theoretical work[27,28] the cohesive energy of ω to be 5 meV/atom lower than α. For Zr the two phases are calculated to be degenerate. For Ni we find in agreement with experiments the γ (fcc) structure to be lowest in energy.

For Zr the cohesive energies is highly accurate—within 0.05 eV/atom of the experimental value—while for the 3*d* transition metals Ti and Ni it is 0.3–0.4 eV/atom too low. These deviations are typically observed for the GGA approximation and largely due to its deficiency for the spin description of the free atom reference states.[38] However, in this work we are interested in the relative stability of the Ti-Zr-Ni phases given by their energy differences. These are significantly more accurate, as will be shown below by comparison with experimental heats of formation of the alloy phases. All lattice parameters are within 1.5% of the experimental values, demonstrating the accuracy of the *ab initio* method for structural properties.

B. Binary Ti-Zr phase diagram

The Ti-Zr phase diagram[39] shows that Ti and Zr are, despite their size difference, completely miscible over the whole composition range. Additionally, CALPHAD fits to thermodynamic data resulted in a zero heat of mixing between the two elements[33] and no ordering transition is known in the Ti-Zr system. Hence, we did not perform calculations for binary Ti-Zr phases.

C. Binary Ti-Ni phase diagram

The Ti-Ni phase diagram shows in addition to the elemental Ti and Ni phases intermetallic compounds with compositions Ti_2Ni, TiNi, and $TiNi_3$.[25,39] The phases δ-Ti_2Ni ($E9_3$) and $TiNi_3$ ($D0_{24}$) are stable over the whole temperature range up to melting.[39] TiNi, on the other hand, shows a martensitic transformation at 903 K from the high-temperature *B*2 phase into the monoclinic *B*19′ phase with an intermediate orthorhombic *R* phase.[29,35,40,41] In addition to the experimentally observed structures, *ab initio* calculations of hypothetical Ti-Ni structures are performed for Ti_3Ni and $TiNi_3$ ($L1_2$), Ti_2Ni (*C*16), TiNi (B_f, *B*19, *B*2, and $L1_0$), Ti_3Ni_4 ($R\bar{3}$), and $TiNi_3$ ($D0_{19}$).

Table II shows the cohesive energies, heats of formation and lattice parameters for the binary Ti-Ni phases. We find in agreement with the experimental phase diagram[39] the ground-state phases δ-Ti_2Ni ($E9_3$), $TiNi_3$ ($D0_{24}$), and *B*19′. The martensite *B*19′ is lower in energy than the high-temperature phase *B*2 and the *R* phase. It relaxes to the higher-symmetry B_f structure. The B_f structure has to our knowledge not been observed, possibly due to high strain. It is also noted that the relaxation to B_f has not been found in earlier work on the *B*19′ phase by Parlinski and Parlinska-Wojtan.[30] Our calculation differ in that we use a higher cutoff energy (400 eV), larger *k*-point meshes and describe the 3*p* electrons as valence electrons. The relaxation to the B_f phase yields an additional energy gain of about 10 meV/atom over the *B*19′ phase with experimental lattice parameters.

D. Binary Zr-Ni phase diagram

The Zr-Ni alloy system exhibits a plethora of phases. The experimental low-temperature phases are Zr_2Ni (*C*16), ZrNi (B_f), Zr_7Ni_{10} (*Aba*2), $ZrNi_3$ ($D0_{19}$), Zr_2Ni_7 (C_2/m), and $ZrNi_5$ ($C15_b$).[39] In Zr-rich alloys a further Zr_7Ni_{10} phase forms with the space group *Pbca*.[25] At high temperatures a Zr_9Ni_{11} phase with space group $I4/m$ and a $ZrNi_2$ *C*15-Laves phase are observed. An additional $Zr_{21}Ni_8$ low-temperature phase occurs at large Ni concentrations.[39] Its structure is as yet unknown. Since the quasicrystal and the competing phases are all forming at low Ni concentrations, no attempt was made to investigate the structure of the $Zr_{21}Ni_8$ phase. In addition to the energies of the experimentally observed Zr-Ni phases, *ab initio* calculations for Zr_3Ni and $ZrNi_3$ ($L1_2$), Zr_2Ni ($E9_3$), as well as ZrNi (*B*19′, *B*19, *R*, and *B*2) are performed.

Table III lists the cohesive energies, heats of formation and lattice parameters of the binary Zr-Ni phases. As-ground state phases we find, in addition to α-Zr (hcp) and γ-Ni (fcc), the phases Zr_2Ni (*C*16), ZrNi (B_f), $ZrNi_3$ ($D0_{19}$), and $ZrNi_5$ ($C15_b$). The Zr_7Ni_{10} phases (*Pbca*) relaxes into the higher symmetry *Aba*2 phase. The calculated energies for both Zr_7Ni_{10} phases *Pbca* and *Aba*2 indicate that these phases are slightly unstable ($\Delta E = 5$ meV/atom) and will decompose into ZrNi and $ZrNi_3$.

Our *ab initio* calculations of the binary Ti-Ni and Zr-Ni ground-state phase diagrams and the heats of formation show excellent agreement with experiment. In most cases the heats of formation agree within about 50 meV/atom with experimental values. Furthermore, our calculated lattice parameters are within 2% of the experimental values for all observed structures.

E. Ternary Ti-Zr-Ni phases

Several experimental studies investigate the properties of ternary Ti-Zr-Ni alloys. Alloys near the composition $Ti_{50}Zr_xNi_{50-x}$ show a reversible martensitic transformation leading to shape-memory behavior.[42] Ternary Zr-based Laves phases have been studied extensively as potential hydrogen storage materials.[43] Properties of crystalline and amorphous structures of the ternary phase diagram along the section Ti_2Ni-Zr_2Ni have been studied by Molokanov *et al.*[44]

In addition to the approximant phase *W*-TiZrNi and the quasicrystal *i*-TiZrNi, three ternary intermetallic TiZrNi phases are known: the hexagonal λ-TiZrNi phase,[32,44] the cubic δ-$(Ti,Zr)_2Ni$ phase,[45,46] and the Ti_2ZrNi_9 phase.[47] The δ phase is stabilized by small amounts of oxygen and is not found in samples low in oxygen;[46] our calculations (Table IV) show it to be unstable with respect to the binary phases. The atomically disordered *C*14 Laves phase λ-TiZrNi is often seen in quasicrystal samples, but is stable only at high temperatures.[13] Total energy calculations for nine deterministic ternary variants of the *C*14 phase showed all to be unstable against decomposition into binary phases, except for the nickel-poor λ-$Ti_6Zr_4Ni_2$; but that in turn is computed to be less stable than the *W*-TiZrNi structure, which has practically the same composition.[32] The crystal structure of the Ni-rich Ti_2ZrNi_9 phase is related to the $TiNi_3$ ($D0_{24}$) and

TABLE II. Structures and electronic energies of the Ti-Ni phases. The cohesive energies E_{coh}, the energy difference to the ground state ΔE, and the heats of formation H_f, are given. Wherever available, experimental values are given in parentheses, taken from Refs. 25, 33, and 35.

Phase	Space group	N_{atoms} Ti	Ni	N_k	E_{coh} in eV/atom	ΔE in meV/atom	H_f in eV/atom	Lattice parameters in Å
Ti_3Ni ($L1_2$)	$Pm\bar{3}m$	3	1	120	5.184	+70	−0.08	a=3.950
Ti_2Ni[a] ($E9_3$)	$Fd\bar{3}m$	16	8	60	5.360	0	−0.29 (−0.28)	a=11.331 (11.324)
Ti_2Ni ($C16$)	$I4/mcm$	4	2	159	5.353	+7	−0.28	a=6.065
								b=4.927
TiNi[a,c] ($B19'$)	$P2_1/m$	2	2	686	5.442	0	−0.42 (−0.35)	a=2.956 (2.884)
								b=4.932 (4.665)
								c=4.013 (4.110)
								γ=106.80° (98.10°)
TiNi (B_f)[c]	$Cmcm$	2	2	512	5.442	0	−0.42	a=4.948
								b=9.444
								c=4.014
TiNi ($B19$)	$Pmma$	2	2	343	5.419	+22	−0.40	a=2.854
								b=4.627
								c=4.176
TiNi (R)	$P3$	9	9	60	5.411	+31	−0.39	a=7.282 (7.358)
								c=5.404 (5.286)
TiNi[b] ($B2$)	$Pm\bar{3}m$	1	1	560	5.391	+50	−0.37 (−0.35)	a=3.021 (3.010)
TiNi[d] ($L1_0$)	$P4/mmm$	2	2	405	5.391	+50	−0.37	a=4.258
								c=3.043
Ti_3Ni_4	$R\bar{3}$	6	8	88	5.432	+10	−0.43	a=6.532
								c=5.054
$TiNi_3$[a] ($D0_{24}$)	$P6_3/mmc$	4	12	80	5.441	0	−0.50 (-0.45)	a=5.126 (5.109)
								c=8.368 (8.319)
$TiNi_3$ ($D0_{19}$)	$P6_3/mmc$	2	6	125	5.426	+15	−0.48	a=5.126
								c=4.185
$TiNi_3$ ($L1_2$)	$Pm\bar{3}m$	1	3	120	5.425	+16	−0.48	a=3.625

[a]Experimentally observed ground-state phase.
[b]Experimentally observed high-temperature phase.
[c]For TiNi the experimentally observed martensitic phase $B19'$ relaxes to the higher-symmetry B_f structure.
[d]The $L1_0$ structure relaxes into the higher-symmetry $B2$ structure.

$ZrNi_3$ ($D0_{19}$) structures.[47] All three structures consist of stackings of hexagonal close-packed (Ti/Zr)Ni_3 layers. The stacking sequence is *ABAC* for $TiNi_3$ ($D0_{24}$), *AB* for $ZrNi_3$ ($D0_{19}$) and *ABABCBCAC* with random Ti and Zr site occupation for Ti_2ZrNi_9.[47] Our calculations placing Zr on the *ABA* layers and Ti on the following *BCBCAC* layers show Ti_2ZrNi_9 to be nearly degenerate with a mixture of $TiNi_3$ ($D0_{24}$) and $ZrNi_3$ ($D0_{19}$). This agrees with the experimental result that Ti and Zr are miscible in these hexagonal close-packed stacking structures.

IV. QUASICRYSTAL PHASE STABILITY

It is nontrivial to calculate the total energy of a quasicrystal, since there is no single finite unit cell. We take advantage of the description of the quasicrystal as a space-filling quasiperiodic tiling of a few types of cell, each type containing a fixed atomic decoration. A *periodic* packing of the same cells forms an "approximant" structure. The total energy of the quasicrystal is estimated by the energy of several approximants.

A. Approximants of the quasicrystal

The first, simpler tiling model[5] uses the "Ammann" cells, a prolate (PR) and oblate (OR) rhombohedron as well as a composite tile called the rhombic dodecahedron (RD), with edge length a_{ico}=5.2 Å. This model's decoration is Ni on vertices, Ti on edges, and Zr (in the role of a larger atom) in interiors. Our Ammann-cell approximants do not contain any icosahedrally symmetric atom clusters and have 4 to 19 atoms per periodic unit cell.

The second tiling model uses larger "canonical cells" known as *A*, *B*, *C*, and *D*.[48] Canonical cell structures can be viewed as a particular way to group Ammann tiles, so as to

TABLE III. Structures and electronic energies of the Zr-Ni phases: The cohesive energies E_{coh}, the energy difference to the ground state ΔE, and the heats of formation H_f are given. Wherever available, experimental values are given in parentheses, taken from Refs. 25 and 33.

Phase	Space group	N_{atoms} Zr	Ni	N_k	E_{coh} in eV/atom	ΔE in meV/atom	H_f in eV/atom	Lattice parameters in Å
Zr_3Ni ($L1_2$)	$Pm\bar{3}m$	3	1	165	5.968	+257	+0.01	a=4.295
Zr_2Ni[a] ($C16$)	$I4/mcm$	4	2	405	6.184	0	−0.33 (−0.38)	a=6.526 (6.483)
								c=5.254 (5.267)
Zr_2Ni ($E9_3$)	$Fd\bar{3}m$	16	8	28	6.091	+93	−0.24	a=12.232
ZrNi[a] (B_f)	$Cmcm$	2	2	343	6.073	0	−0.46 (−0.51)	a=3.311 (3.267)
								b=10.057 (9.903)
								c=4.097 (4.107)
ZrNi ($B19'$)	$P2_1/m$	2	2	432	6.073	0	−0.46	a=3.317
								b=4.082
								c=5.286
								γ=108.00°
ZrNi ($B19$)	$Pmma$	2	2	343	5.997	+76	−0.39	a=3.197
								b=4.251
								c=4.986
ZrNi (R)	$P3$	9	9	108	5.967	+106	−0.36	a=7.789
								c=5.745
ZrNi ($B2$)		1	1	560	5.965	+108	−0.36	a=3.223
Zr_9Ni_{11}[b]	$I4/m$	9	11	52	5.924	+75	−0.39	a=10.044 (9.88)
								c=6.492 (6.61)
Zr_3Ni_4	$R\bar{3}$	6	8	88	5.944	+23	−0.44	a=7.002
								b=6.064
								c=1.751
Zr_7Ni_{10}[a]	$Aba2$	14	20	12	5.936	+6	−0.46 (−0.54)	a=9.227 (9.211)
								b=9.226 (9.156)
								c=12.476 (12.386)
Zr_7Ni_{10}[a]	$Pdca$	28	40	8	5.936	+6	−0.46 (−0.54)	a=9.230 (9.325)
								b=9.213 (9.210)
								c=12.488 (12.497)
$ZrNi_2$[b] ($C15$)	$Fd\bar{3}m$	2	4	110	5.771	+55	−0.41 (−0.73)	a=7.003 (6.916)
$ZrNi_3$[b] ($D0_{19}$)	$P6_3/mmc$	2	6	343	5.702	0	−0.46 (−0.69)	a=5.345 (5.309)
								c=4.330 (4.303)
$ZrNi_3$ ($L1_2$)	$Pm\bar{3}m$	1	3	220	5.661	+41		a=3.771
Zr_2Ni_7[a]	C_2/m	4	14	144	5.627	0	−0.43 (−0.48)	a=4.694 (4.698)
								b=8.275 (8.235)
								c=12.210 (12.193)
$ZrNi_5$[a] ($C15_b$)	$F\bar{4}3m$	1	5	182	5.435	+3	−0.32 (−0.36)	a=6.734 (6.702)

[a]Experimentally observed ground-state phase.
[b]Experimentally observed high-temperature phase.

maximize the frequency of the icosahedrally symmetric 45-atom "Bergman cluster." The cluster centers are the corners of the canonical cells, linked by edges of 12.4 Å length. This model's atomic decoration is locally similar to the first model's, but permits many more site types depending on the local context. The canonical-cell approximants (A_6, B_2C_2, and D_2 packings) are relatively large, with 81 to 123 atoms per crystallographic unit cell.[11,48]

In a previous paper, we determined the structure of *i*-TiZrNi by a constrained least-squares fit of the canonical cell model.[11] The chemical site occupations were refined using x-ray and neutron-diffraction data, while the atomic positions were optimized by *ab initio* relaxations of the resulting atomic decoration for periodic tilings; two iterations of this two-step procedure gave convergence. Several sites were found to have mixed occupation, which must be chosen one

TABLE IV. Structures and electronic energies of the Ti-Zr-Ni phases: The cohesive energies E_{coh}, the energy difference to the mixture of the competing binary ground state phases ΔE, and the heats of formation H_f are given. Wherever available, experimental values are given in parentheses, taken from Refs. 25 and 33.

Phase	Space group	N_{atoms} Ti	Zr	Ni	N_k	E_{coh} in eV/atom	ΔE in meV/atom	H_f in eV/atom	Lattice parameters in Å
δ-$Ti_6Zr_2Ni_4$ ($E9_3$)	$Fd\bar{3}m$	12	4	8	28	5.497	+70	−0.23	a=11.665
δ-$Ti_2Zr_6Ni_4$ ($E9_3$)	$Fd\bar{3}m$	4	12	8	28	5.937	+42	−0.28	a=11.952
λ-$Ti_4Zr_4Ni_4^b$ ($C14$)	$P3m1$	4	4	4	88	5.638	+136	−0.17	a=5.277 (5.23)
									c=8.382 (8.55)
λ-$Ti_6Zr_4Ni_2$ ($C14$)	$P6_3/mmc$	6	4	2	60	5.688	−8	−0.17	a=5.638
									c=7.897
Ti_2ZrNi_9	$R\bar{3}m$	6	3	27	10	5.513	+1	−0.47	a=5.196 (5.157)
									c=19.10 (18.89)

way or the other in the *ab initio* calculations, producing the numbered variant decorations in Table V.

B. Energies of the approximants

Table V shows the energies and lattice parameters of the approximant structures and Fig. 1 shows the ternary ground state phase diagram. For the approximants the ternary ground-state energy surface is constructed the same way as for the binary phases: The energy difference ΔE is calculated between each approximant and the phase mixture (of up to three phases) with the same composition and the lowest possible energy; for ground-state structures $\Delta E=0$. Similarly, to compare with the binary phases, ΔE_{binary} is defined relative to a phase mixture of three competing binary phases. Depending on the composition of the approximant, the competing binary phases are α-Ti, Zr_2Ni, and either α-Zr or ZrNi. Similarly, in experiments at about 500 °C the competing phases of the quasicrystal are α-Ti/Zr, Ti_2Ni, Zr_2Ni, λ-TiZrNi (Laves phase), and the *W*-TiZrNi approximant phase.[13]

Of the three Ammann approximants, the OR and the RD are unstable against the competing binary phases. The PR packing is stable against the binary phases but unstable against the larger canonical cell approximants. The low energy of the PR structure can be understood by its similarity to the cubic $C15$ $ZrNi_2$ Laves phase;[5] it can be obtained from the $ZrNi_2$ structure by replacing most of the Ni atoms with Ti.

The canonical cell approximants, on the other hand, have significantly lower energies. They are all stable against the competing binary phases by 8 to 24 meV/atom and lower in

TABLE V. Electronic energies of periodic tiling structures approximating *i*-TiZrNi. Energies E, energy differences to the ground state ΔE, and to the binary phases ΔE_{binary} are given. The relaxed icosahedral lattice parameter a_{ico} of the approximant structures resembles closely the experimental value of the quasicrystal of 5.16 Å (Ref. 12). Two models for the quasicrystal are constructed from (a) $A_6^{(1)}+B_2C_2^{(1)}+D_2^{(1)}$ and (b) $A_6^{(1)}+B_2C_2^{(2)}+D_2^{(1)}$. For comparison, the quasicrystal has an experimental composition of $Ti_{41.5\pm1}Zr_{41.5\pm1}Ni_{17}$.

Structure	N_{atoms} Ti	Zr	Ni	N_k	E_{coh} in eV/atom	ΔE in meV/atom	ΔE_{binary} in meV/atom	a_{ico} in Å
OR	3	0	1	146	4.989	+326	+326	5.25
PR	3	2	1	146	5.685	+15	−5	5.14
RD	8	8	3	14	5.688	+110	+84	5.39
$A_6^{(1)}$	36	32	13	4	5.770	0	−22	5.23
$A_6^{(2)}$	42	26	13	4	5.682	0	−20	5.19
$A_6^{(3)}$	48	20	13	4	5.594	0	−24	5.16
$B_2C_2^{(1)}$	42	34	15	6	5.741	+4	−19	5.23
$B_2C_2^{(2)}$	36	40	15	6	5.811	+9	−11	5.27
$B_2C_2^{(3)}$	44	32	15	6	5.715	+4	−19	5.22
$D_2^{(1)}$	60	42	21	4	5.701	+10	−9	5.22
$D_2^{(2)}$	62	40	21	4	5.678	+15	−8	5.21
i-TiZrNi (a)	46.0%	37.6%	16.4%		5.744	+3	−18	5.23
i-TiZrNi (b)	42.7%	40.9%	16.4%		5.779	+6	−14	5.25

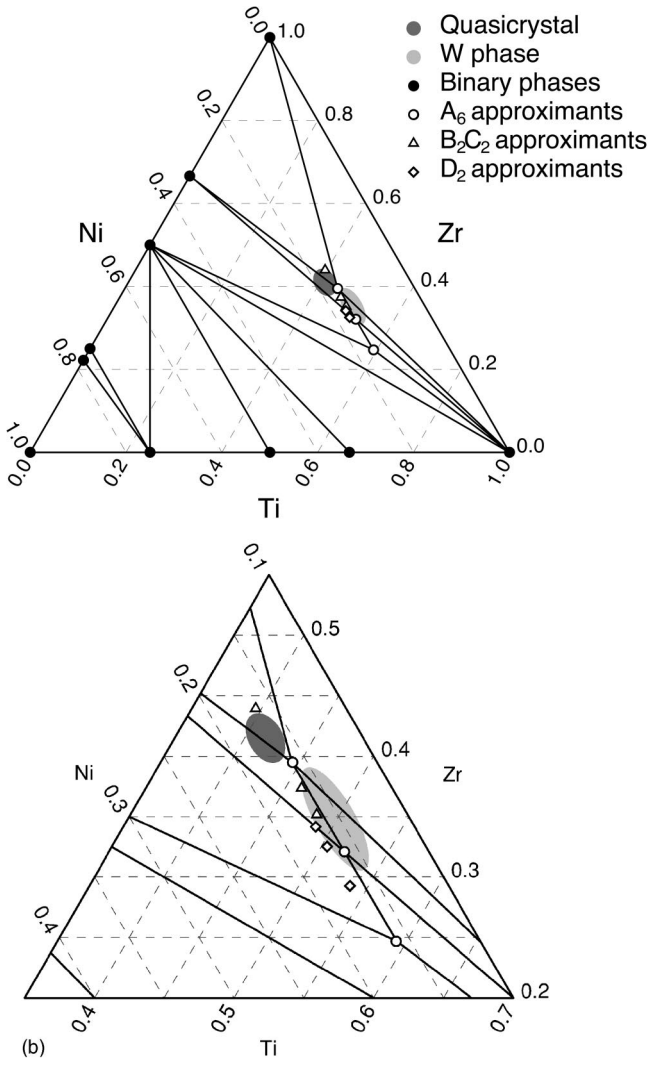

FIG. 1. Ground-state phase diagram of Ti-Zr-Ni showing the creases (solid lines) of the minimum energy surface of the competing phases. Each crease represents a domain of coexistence of the two phases at that crease's end points. Each three-phase coexistence domain is a triangle bounded by creases with end points at the corresponding single-phase points. Shaded regions represent the experimental composition of the quasicrystal and the approximant phase.

energy than the ternary λ-$Ti_6Zr_4Ni_2$ phase and the PR approximant, as mentioned earlier.

The three A_6 structures are ground-state structures. The A_6 approximants corresponds to the experimentally observed *W*-TiZrNi phase which inspired the structure model.[11] Diffraction experiments show that *W*-TiZrNi has Ti/Zr disorder on the two sites which lie on the plane bisecting the axis linking two Bergman clusters.[17] Different chemical occupations of these "glue" sites by Ti and Zr result in the variants $A_6^{(1)}$, $A_6^{(2)}$, and $A_6^{(3)}$. All three structures are ground states for their composition and form a line on the ground-state energy surface, indicating that Ti/Zr disorder on these sites costs zero energy.

The next larger canonical cell approximants B_2C_2 and D_2 do not correspond to experimentally observed phases. They are stable with respect to the binary phases but are slightly higher in energy than the A_6 approximants: They lie within 4 to 15 meV/atom of the ground-state energy surface. We investigate variant site occupations in the B_2C_2 and D_2 approximants.[49] Changing Zr atoms to Ti on certain sites only weakly influences the energy, whereas changing Ti atoms to Ni leads to a significant increase of the energy, indicating that the quasicrystal contains Ti/Zr disorder but no Ti/Ni disorder, in agreement with the structural refinement of *i*-TiZrNi.[11]

Decorations of all three quasicrystal-like canonical cell approximants are stable against the competing binary phases. The three A_6 approximants are the most stable followed by the larger B_2C_2 and D_2 approximants. The stability of the decoration model of the three periodic canonical cell tilings is a strong indication that the decoration of a larger tiling is stable and supports our atomic decoration model.[11]

C. Energy of the quasicrystal

We estimate the energy of the *i*-TiZrNi quasicrystal by summing the energies of each constituent tile, as found from the approximant structures. In an infinite icosahedral canonical-cell tiling the ratio of the canonical cells is constrained by the icosahedral symmetry such that the *BC* cells occupy half the volume.[48] The ratio of the remaining *A* and *D* cells is a free parameter. We adopt the so-called "magic" value $\zeta = 3(1-2/\sqrt{5}) \approx 0.32$ for the volume ratio of *D* to *A* cells (see Sec. V C of Ref. 48). The magic ζ value is plausible because (i) it favors the lower energy *A* cells, (ii) it is close to the value that maximizes the entropy of possible tilings,[50] and (iii) the density of Bergman cluster center is such that it might be specified by a simple acceptance domain.[51] The resulting number ratio of cells is $N(A):N(BC):N(D) = 3[3-\sqrt{5}]:1:[\sqrt{5}-2]$.

Taking the lowest-energy tiling structures $A_6^{(1)}$, $B_2C_2^{(1)}$, and the $D_2^{(1)}$ yields for the composition of the quasicrystal model (a) $Ti_{46.0}Zr_{37.6}Ni_{16.4}$, 4% higher in Ti and lower in Zr than the experimental composition of $Ti_{41.5\pm1}Zr_{41.5\pm1}Ni_{17}$. Taking the Zr rich $B_2C_2^{(2)}$ structure instead yields model (*b*) $Ti_{42.7}Zr_{40.9}Ni_{16.4}$ within 1% of the experimental composition.

The lattice parameters of the canonical cells composing the quasicrystal models are very similar. They range from 5.22−5.23 Å for model (a) and 5.22−5.27 Å for model (b). This results in negligible strains in the quasicrystalline packing of the cells. The quasicrystal lattice parameter is estimated by averaging the values for the canonical cells according to their volume fraction. The predicted lattice parameters of the quasicrystal are 5.23 Å for model (a) and 5.25 Å for model (b), close to the experimental value of 5.16 Å.[12]

The energy of the quasicrystal is estimated by averaging the energies of the canonical cell approximants according to their number ratio neglecting intertile interactions.[52] The quasicrystal models are 14 to 18 meV/atom lower in energy than the competing binary phases, the λ-$Ti_6Zr_4Ni_2$ phase and the PR approximant.

The quasicrystal models are close in energy to the *W* phase corresponding to the A_6 approximants. Our calculations imply an energy difference favoring the *W* phase over

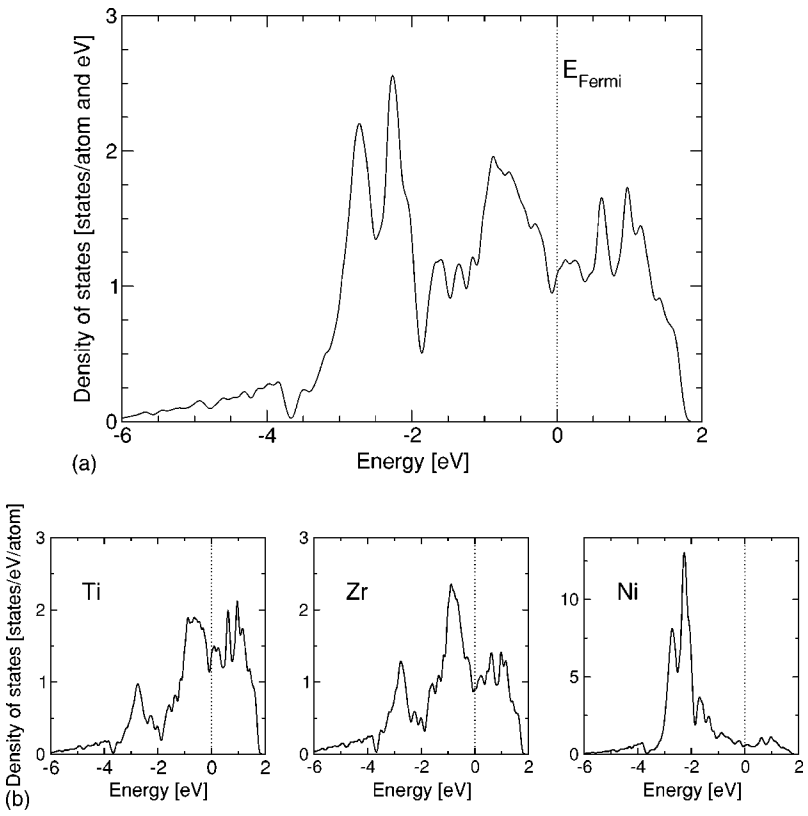

FIG. 2. Density of states of the 1/1 approximant *W*-TiZrNi: (a) total density of states and (b) partial site-projected density of states. The densities are smoothed using a Gaussian with $\sigma = 50$ meV corresponding to a Fermi-Dirac distribution of ambient temperature. The energy is measured relative to the Fermi energy.

the quasicrystal by 3 to 6 meV/atom. However, these energy differences are below the limit of accuracy of the *ab initio* method. Furthermore, intertile interactions, which were hitherto neglected, and the removal of the periodicity constraints in the quasicrystal allowing for additional relaxations could further stabilize the quasicrystal models.

Energy calculations for larger approximants would permit the extraction of the "tile Hamiltonian," whereby energy differences are written as a sum of single tile and intertile interactions.[52,53] Our result, that different tilings are nearly degenerate, is the prerequisite for any model of quasicrystal long-range order which treats the tiles as degrees of freedom. If the intertile interactions are small compared to the melting temperature, the quasicrystal phase could be stabilized at hightemperatures by entropy. If the intertile interactions were such as to implement matching rules or maximize the density of certain local patterns,[54] then a nonrandom quasicrystal could be stabilized at low temperatures. Our calculations do not address the intertile interactions which would reqire larger system sizes.

The long-time annealing experiments and the observed phase transition between the *W* phase and the quasicrystal demonstrate that the *i*-TiZrNi quasicrystal is lower in energy than the *W* approximant. We find the quasicrystal and the *W* phase to be close in energy and both to be stable with respect to the other competing phases. Combining the experimental results and our calculations suggests that the *i*-TiZrNi is a ground-state quasicrystal.

D. Electronic structure and stabilization of *i*-TiZrNi

The energetic stability of metallic alloys is determined by atomic size mismatch and the chemical interactions between the alloy components. The electronic density of states (DOS) of a material and the charge transfer between its alloy components are fingerprints of its electronic structure and provide insight into the stabilization mechanisms. For transition metal compounds the DOS is largely determined by the local atomic structure. Furthermore the electronic densities of states are experimentally accessible by a number of techniques, such as photoemission and absorption spectroscopy[55] as well as specific heat measurements.

The DOS of the *i*-TiZrNi quasicrystal is estimated by averaging the DOS of the A_6, B_2C_2, and D_2 approximants according to their number ratio in the quasicrystal structure. Since the local structure in all three approximants is very similar, intertile interactions are not expected to change the electronic structure in the quasicrystal considerably. The DOS are calculated using $8\times8\times8$, $6\times6\times6$, and $3\times3\times3$ *k*-point meshes for the A_6, the B_2C_2, and the D_2 approximants. For large structures the finite number of *k* points usually results in artificial spikes in the DOS.[56–60] To avoid the spikes, the DOS are smoothed by a Gaussian, with $\sigma = 50$ meV, resembling the Fermi-Dirac distribution at ambient temperature.

Figures 2 and 3 show the DOS of the approximant *W*-TiZrNi and the *i*-TiZrNi quasicrystal. The DOS of the quasicrystal is very similar to the one of the *W* phase, reflecting the similarities of the atomic structure. The DOS is dominated by a 6 eV wide *d*-band complex, which is structured into a number of subbands. The *d* states of the Ni atoms 2 to 3 eV below the Fermi level are well separated from the *d* states of the Ti and Zr atoms around the Fermi level. The central minimum in the density of states around -1.9 eV is formed by hybridization of the Ti/Zr and Ni dominated subbands.[61]

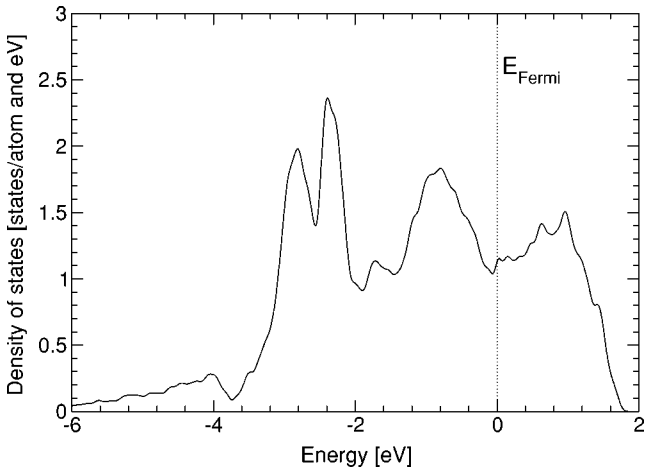

FIG. 3. Density of states of the icosahedral TiZrNi quasicrystal obtained by averaging over the density of states of the A_6, B_2C_2, and D_2 tiling and smoothed using a Gaussian with $\sigma = 50$ meV.

In real space the hybridization corresponds to charge transfer from the Ti and Zr to Ni. Bader analysis[62] determines the charge transfer in the approximant structures of Table V. Ti transfers 1.5 electrons and Zr 0.5 electrons to Ni gaining 1.8 electrons. A similar charge transfer is observed for the binary Ti-Ni and Zr-Ni phases. The large charge transfer from the Ti and Zr atoms to Ni is consistent with the higher electronegativity of Ni (1.75) as compared to Ti (1.32) and Zr (1.22).[63]

The DOS shows a minimum around the Fermi level, with the smallest value of the density of states about 0.1 eV below the Fermi energy. In general, one expects a reduction of the DOS near the Fermi level to provide a stabilizing contribution to the electronic energy.[64] The stabilizing effects of a Fermi-level gap are apparent in covalently bonded materials, which have both strong bonds and band gaps. A full gap does not exist in metallic compounds. However, the "pseudogap" at the Fermi level, as observed here and often found in quasicrystals[59] and intermetallic compounds, contains in partial fashion the stabilizing effect of the gap.[64] The stabilization effect here is similar to the mechanism suggested by Turchi and Ducastelle[65,66] as well as Pettifor and Aoki,[67] where the differences in the electronic density of states determine the relative stabilities of crystalline phases.

The charge transfer from Ti and Zr to Ni and the hybridization between the Ti/Zr and Ni bands result in a strong attractive interaction between Ti/Zr and Ni. Thus, it is energetically favorable for Ni to be surrounded by Ti and Zr. This explains why in the quasicrystalline structure the Ni atoms occupy the corner sites of the Ammann tiles surrounded by Ti and Zr.[11] Furthermore, since Zr is slightly larger than Ti it is no surprise that Zr occupies the more open sites of the structure. However, the unstable small Ammann approximants PR, OR, and RD have similar local atomic structure as the canonical-cell approximants A_6, B_2C_2, and D_2. The main difference is that complete Bergman clusters are absent in the small Ammann approximants, but dense in the canonical cell approximants where they contain about half of the atoms. We conjecture that the presence of Bergman cluster in the canonical cells is responsible for the stability.

V. CONCLUSION

Ab initio methods determine the stability of the icosahedral TiZrNi quasicrystal by calculating the complete Ti-Zr-Ni ground-state phase diagram. For the binary phases, the calculated heats of formation agree with experimental values within 50 meV/atom and the lattice parameters within 2%, demonstrating the accuracy of the *ab initio* method. The structure of the *i*-TiZrNi quasicrystal is modeled by an atomic decoration of canonical cells.[11] The energy of the quasicrystal is estimated from the energy of several periodic approximants neglecting intertile interactions. Using the lowest-energy approximant structures predicts the composition of the quasicrystal within 4% of the experiment and the lattice parameter within 2%. The quasicrystal model and the *W*-approximant phase are similar in energy and both about 20 meV/atom lower in energy than the competing phases. Combining the experimental result that the quasicrystal is lower in energy than the *W* phase with our calculation showing that both phases are stable with respect to competing phases suggests that the icosahedral TiZrNi quasicrystal is a ground-state quasicrystal.

ACKNOWLEDGMENTS

The work at Washington University was supported by the National Science Foundation (NSF) under Grants Nos. DMR 97-05202 and DMR 00-72787. C.L.H. was supported by DOE Grant DE-FG02-89ER-45405. R.G.H. was partially supported by NSF Grant No. DMR-0080766, DOE Grant No. DE-FG02-99ER45795, and the Washington University grants. Calculations were performed at the Ohio Supercomputer Center and NERSC.

[1] D. Shechtman, I. Blech, D. Gratias, and J. W. Cahn, Phys. Rev. Lett. **53**, 1951 (1984).
[2] A. P. Tsai, A. Inoue, Y. Yokoyama, and T. Masumoto, Mater. Trans., JIM **31**, 98 (1990).
[3] Y. Yokoyama, T. Miura, A.-P. Tsai, A. Inoue, and T. Masumoto, Mater. Trans., JIM **33**, 97 (1992).
[4] C. Janot, M. de Boissieu, M. Boudard, H. Vincent, M. Durand, and J. M. Dubois, J. Non-Cryst. Solids **150**, 322 (1992).
[5] C. L. Henley and V. Elser, Philos. Mag. B **53**, L59 (1986).
[6] A. P. Tsai, A. Niikura, A. Inoue, T. Masumoto, Y. Nishida, K. Tsuda, and M. Tanaka, Philos. Mag. Lett. **70**, 169 (1994).
[7] I. R. Fisher, Z. Islam, A. F. Panchula, K. O. Cheon, M. J. Kramer, P. C. Canfield, and A. I. Goldman, Philos. Mag. B **77**, 1601 (1998).
[8] X. Zhang and K. F. Kelton, Philos. Mag. Lett. **62**, 265 (1990).
[9] J. L. Libbert and K. F. Kelton, Philos. Mag. Lett. **71**, 153 (1995).
[10] R. G. Hennig and H. Teichler, Philos. Mag. A **76**, 1053 (1997).
[11] R. G. Hennig, K. F. Kelton, A. E. Carlsson, and C. L. Henley,

Phys. Rev. B **67**, 134202 (2003).
[12] K. F. Kelton, W. J. Kim, and R. M. Stroud, Appl. Phys. Lett. **70**, 3230 (1997).
[13] J. P. Davis, E. H. Majzoub, J. M. Simmons, and K. F. Kelton, Mater. Sci. Eng., A **294-296**, 104 (2000).
[14] P. C. Gibbons and K. F. Kelton, in *Physical Properties of Quasicrystals*, Vol. 126 of *Solid State Sciences*, edited by Z. M. Stadnik (Springer, Berlin, 1999), pp. 403-431.
[15] R. M. Stroud, A. M. Viano, P. C. Gibbons, K. F. Kelton, and S. T. Misture, Appl. Phys. Lett. **69**, 2998 (1996).
[16] W. J. Kim, P. C. Gibbons, and K. F. Kelton, Philos. Mag. Lett. **76**, 199 (1997).
[17] R. G. Hennig, E. H. Majzoub, A. E. Carlsson, K. F. Kelton, C. L. Henley, W. B. Yelon, and S. Misture, Mater. Sci. Eng., A **294-296**, 361 (2000).
[18] S. Yi and D. H. Kim, J. Mater. Res. **15**, 892 (2000).
[19] G. Kresse and J. Hafner, Phys. Rev. B **47**, R558 (1993).
[20] G. Kresse and J. Furthmüller, Phys. Rev. B **54**, 11 169 (1996).
[21] D. Vanderbilt, Phys. Rev. B **41**, R7892 (1990).
[22] G. Kresse and J. Hafner, J. Phys.: Condens. Matter **6**, 8245 (1994).
[23] J. P. Perdew, in *Electronic Structure of Solids '91*, edited by P. Ziesche and H. Eschrig (Akademie Verlag, Berlin, 1991), p. 11.
[24] P. E. Blöchl, O. Jepsen, and O. K. Andersen, Phys. Rev. B **49**, 16 223 (1994).
[25] P. Villars and L. D. Calvert, *Pearson's Handbook of Crystallographic Data for Intermetallic Phases*, 2nd ed. (American Society for Metals, Metals Park, Ohio, 1991).
[26] R. Ahuja, J. M. Wills, B. Johansson, and O. Eriksson, Phys. Rev. B **48**, 16 269 (1993).
[27] D. R. Trinkle, R. G. Hennig, S. G. Srinivasan, D. M. Hatch, M. D. Jones, H. T. Stokes, R. C. Albers, and J. W. Wilkins, Phys. Rev. Lett. **91**, 025701 (2003).
[28] A. L. Kutepov and S. G. Kutepova, Phys. Rev. B **67**, 132102 (2003).
[29] M. Sanati, R. C. Albers, and F. J. Pinski, Phys. Rev. B **58**, 13 590 (1998).
[30] K. Parlinski and M. Parlinska-Wojtan, Phys. Rev. B **66**, 064307 (2002).
[31] A. Pasturel, C. Colinet, D. N. Manh, A. T. Paxton, and M. van Schilfgaarde, Phys. Rev. B **52**, 15 176 (1995).
[32] E. H. Majzoub, R. G. Hennig, and K. F. Kelton, Philos. Mag. Lett. **83**, 65 (2003).
[33] F. R. de Boer, R. Boom, W. C. M. Mattens, A. R. Miedema, and A. K. Niessen, *Cohesion in Metals: Transition Metal Alloys*, Vol. 1 of *Cohesion and Structure* (North-Holland, Amsterdam, 1988).
[34] S. K. Sikka, Y. K. Vohra, and R. Chidambaram, Prog. Mater. Sci. **27**, 245 (1982).
[35] T. Hara, T. Ohba, E. Okunishi, and K. Otsuka, Mater. Trans., JIM **38**, 11 (1997).
[36] J. C. Jamieson, Science **140**, 72 (1963).
[37] S. P. Rudin, M. D. Jones, and R. C. Albers, Phys. Rev. B **69**, 094117 (2004).
[38] P. H. T. Philipsen and E. J. Baerends, Phys. Rev. B **54**, 5326 (1996).
[39] T. B. Massalski, *Binary Alloy Phase Diagrams* (The Materials Information Society, Materials Park, Ohio, 1990).
[40] M. J. Marcinkowski, A. S. Sastri, and D. Koskimaki, Philos. Mag. **18**, 945 (1968).
[41] K. Otsuka, T. Sawamura, and K. Shimizu, Phys. Status Solidi A **5**, 457 (1971).
[42] S. F. Hsieh and S. K. Wu, J. Alloys Compd. **266**, 276 (1998).
[43] M. Bououdina, H. Enoki, and E. Akiba, J. Alloys Compd. **281**, 290 (1998).
[44] V. V. Molokanov, V. N. Chebotnikov, and Y. K. Kovneristyi, Inorg. Mater. **25**, 46 (1989).
[45] G. A. Yurko, J. W. Barton, and F. G. Parr, J. Appl. Crystallogr. **12**, 909 (1959).
[46] R. Mackay, G. J. Miller, and H. F. Franzen, J. Alloys Compd. **204**, 109 (1994).
[47] J. L. Glimois, P. Forey, R. Guillen, and J. L. Feron, J. Less-Common Met. **134**, 221 (1987).
[48] C. L. Henley, Phys. Rev. B **43**, 993 (1991).
[49] R. G. Hennig, Ph.D. thesis, Washington University, St. Louis, 2000.
[50] M. Mihalkovič and C. L. Henley (unpublished)
[51] P. Kalugin, Europhys. Lett. **9**, 545 (1989).
[52] M. Mihalkovic, W. J. Zhu, C. L. Henley, and R. Phillips, Phys. Rev. B **53**, 9021 (1996).
[53] M. Mihalkovic, W. J. Zhu, C. L. Henley, and M. Oxborrow, Phys. Rev. B **53**, 9002 (1996).
[54] H.-C. Jeong and P. J. Steinhardt, Phys. Rev. Lett. **73**, 1943 (1994).
[55] E. Belin-Ferre, R. G. Hennig, Z. Dankhazi, A. Sadoc, J. Y. Kim, and K. F. Kelton, J. Alloys Compd. **342**, 337 (2002).
[56] R. Haerle and P. Kramer, Phys. Rev. B **58**, 716 (1998).
[57] T. Fujiwara, in *Physical Properties of Quasicrystals*, edited by Z. M. Stadnik Vol. 126 of *Springer Series in Solid-State Science* (Springer, Berlin, 1999), Chap. 6, pp. 169–207.
[58] J. Hafner and M. Krajči, in *Physical Properties of Quasicrystals* (Ref. 57) Chap. 7, pp. 209–256.
[59] Z. M. Stadnik, in *Physical Properties of Quasicrystals*, edited by Z. M. Stadnik, Vol. 126 of *Springer Series in Solid-State Sciences* (Springer, Berlin, 1999) Chap. 8, pp. 257–293.
[60] E. S. Zijlstra and T. Janssen, Europhys. Lett. **52**, 578 (2000).
[61] C. Hausleitner and J. Hafner, Phys. Rev. B **45**, 115 (1992).
[62] R. F. W. Bader, *Atoms in Molecules-A Quantum Theory* (Oxford University Press, Oxford, 1990).
[63] F. A. Cotton and G. Wilkinson, *Inorganic Chemistry*, 3rd ed. (John Wiley, New York, 1972).
[64] A. E. Carlsson and P. J. Meschter, in *Intermetallic Compounds. Principles and Practice*, edited by J. H. Westbrook and R. L. Fleischer (Wiley and Sons, New York, 1995), Vol. 1, Chap. 3, pp. 55–76.
[65] P. Turchi and F. Ducastelle, in *The Recursion Method and Its Applications*, edited by D. G. Pettifor and D. L. Weaire, Vol. 58 of *Springer Series in Solid-State Sciences* (Springer, Berlin, 1985), pp. 104–119.
[66] F. Ducastelle, *Order and Phase Stability in Alloys*, Vol. 3 of *Cohesion and Structure* (North-Holland, Amsterdam, 1991).
[67] D. G. Pettifor and M. Aoki, Philos. Trans. R. Soc. London, Ser. A **334**, 439 (1991).